Inorganic Chemistry

Article

pubs.acs.org/IC

Detailed Mechanism of Phosphoanhydride Bond Hydrolysis Promoted by a Binuclear Zr^{IV}-Substituted Keggin Polyoxometalate Elucidated by a Combination of ^{31}P, ^{31}P DOSY, and ^{31}P EXSY NMR Spectroscopy

Thi Kim Nga Luong,[†] Pavletta Shestakova,*[,†,‡] Gregory Absillis,[†] and Tatjana N. Parac-Vogt*[,†]

[†]Laboratory of Bioinorganic Chemistry, Department of Chemistry, KU Leuven, Celestijnenlaan 200F, 3001 Leuven, Belgium

[‡]NMR Laboratory, Institute of Organic Chemistry with Centre of Phytochemistry Bulgarian Academy of Sciences, Acad. G. Bontchev Str., B1.9, 1113 Sofia, Bulgaria

Supporting Information

ABSTRACT: A detailed reaction mechanism is proposed for the hydrolysis of the phosphoanhydride bonds in adenosine triphosphate (ATP) in the presence of the binuclear Zr^{IV}-substituted Keggin type polyoxometalate $(Et_2NH_2)_8[\{\alpha\text{-}PW_{11}O_{39}Zr(\mu\text{-}OH)(H_2O)\}_2]\cdot 7H_2O$ (ZrK 2:2). The full reaction mechanism of ATP hydrolysis in the presence of ZrK 2:2 at pD 6.4 was elucidated by a combination of ^{31}P, ^{31}P DOSY, and ^{31}P EXSY NMR spectroscopy, demonstrating the potential of these techniques for the analysis of complex reaction mixtures involving polyoxometalates (POMs). Two possible parallel reaction pathways were proposed on the basis of the observed reaction intermediates and final products. The 1D ^{31}P and ^{31}P DOSY spectra of a mixture of 20.0 mM ATP and 3.0 mM ZrK 2:2 at pD 6.4, measured immediately after sample preparation, evidenced the formation of two types of complexes, I1A and I1B, representing different binding modes between ATP and the Zr^{IV}-substituted Keggin type polyoxometalate (ZrK). Analysis of the NMR data shows that at pD 6.4 and 50 °C ATP hydrolysis in the presence of ZrK proceeds in a stepwise fashion. During the course of the hydrolytic reaction various products, including adenosine diphosphate (ADP), adenosine monophosphate (AMP), pyrophosphate (PP), and phosphate (P), were detected. In addition, intermediate species representing the complexes ADP/ZrK (I2) and PP/ZrK (I5) were identified and the potential formation of two other intermediates, AMP/ZrK (I3) and P/ZrK (I4), was demonstrated. ^{31}P EXSY NMR spectra evidenced slow exchange between ATP and I1A, ADP and I2, and PP and I5, thus confirming the proposed reaction pathways.

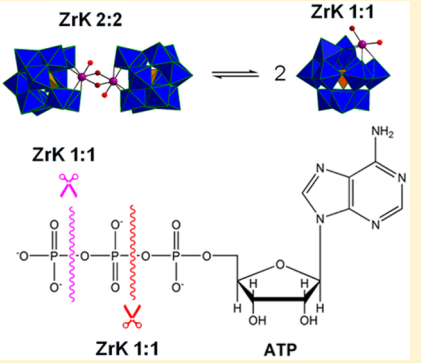

INTRODUCTION

Adenosine triphosphate (ATP, Figure 1) plays an important role in energy transformation in all living organisms, as it is the center for chemical energy storage through its triphosphate chain.[1−3] The hydrolysis of ATP to adenosine diphosphate (ADP, Figure 1) and phosphate (P, Figure 1) is associated with release of energy, which is an important driving force for metabolic processes in living cells.[4] For example, protein degradation in animal and bacterial cells is dependent upon ATP, and ATP hydrolysis is required for the degradation of proteins to acid-soluble products. Moreover, ATP consumption may promote the release of the polypeptide product from the enzyme and, alternatively, ATP hydrolysis may permit the translocation of the enzyme along the substrate to the next cleavage site.[5] In addition, ATP hydrolysis via highly efficient metalloenzymatic ATPases also plays a central role in a variety of processes including photosynthesis phosphorylation, oxidative phosphorylation, and muscle action.[6]

Uncatalyzed ATP hydrolysis in aqueous solution is a slow process with a half-life between 10 and 100 days in the pH range 1−12 at room temperature.[7] However, the rate of ATP hydrolysis is increased by a factor of 10^{11} via enzymatic catalysis and a factor of 10−100 in the presence of metal ions.[7] As a result, natural phosphatase enzymes play an important role in various biotechnology applications. For example, alkaline phosphatases isolated from mammals are used to hydrolyze or transphosphorylate numerous phosphate compounds in vitro.[8] Alkaline phosphatases isolated from mouse intestine are able to catalyze the synthesis of inorganic pyrophosphate from inorganic phosphate during the hydrolysis of glucose 6-phosphate, ATP, ADP, or *p*-nitrophenyl phosphate.[9] Unfortunately natural phosphatases with high purity are not easy to obtain, and the enzymatic properties of these enzymes are affected by activators and inhibitors such as amino acids and metal ions in varying concentrations.[10]

Alternatively, due to their selectivity and efficiency, artificial phosphatases can be used for the hydrolysis of substrate phosphoester bonds.[11−13] Such compounds can be synthesized in large amounts, and their structures can be tuned and designed depending on the specific purpose.[14,15] Moreover, their use may help in understanding the precise role that active

Received: February 16, 2016

DOI: 10.1021/acs.inorgchem.6b00385
Inorg. Chem. XXXX, XXX, XXX−XXX

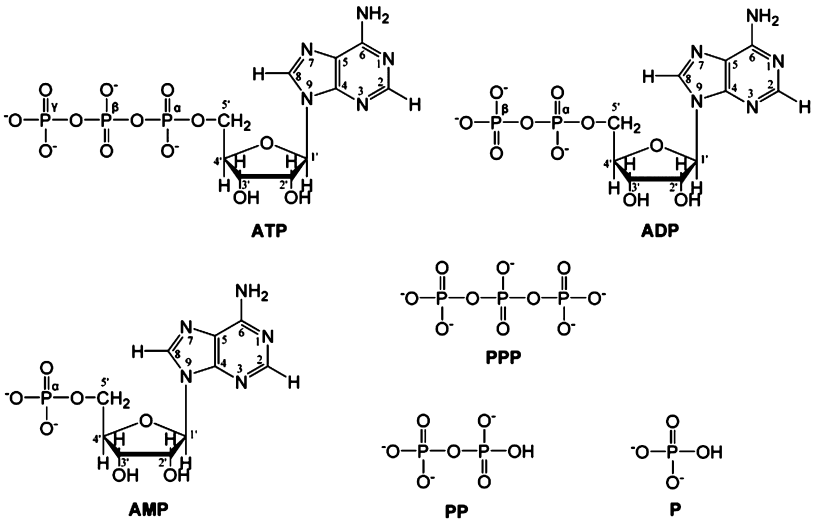

Figure 1. Structures of adenosine triphosphate (ATP), adenosine diphosphate (ADP), adenosine monophosphate (AMP), triphosphate (PPP), pyrophosphate (PP), and phosphate (P).

metal ions play in natural phosphatases.[11] Several studies demonstrated the important role of metal ions as well as their complexes in ATP hydrolysis. For example, in the presence of Cu^{2+},[16] VO_2^+ and VO^{2+} and oxidants,[7] and the Co^{III} complex[17] $[tn_2Co^{III}(OH_2)_2]$ (tn = trimethylenediamine) the rate of ATP hydrolysis increases up to factors of 530, 10^4, and 10^5, respectively, in comparison with pure ATP hydrolysis. The increase in ATP hydrolysis reaction rate in the presence of metal centers can be explained by various factors, including an increase in the reactivity of the phosphorus centers toward the incoming nucleophile due to the electron-withdrawing character of the metal centers, activation and/or delivery of the nucleophile, and/or stability of the pentacoordination transition state and the leaving group.[17−19]

Recent studies in our group demonstrated unprecedented phosphoesterase activity of several metal-substituted polyoxometalates (POMs).[15,20−22] POMs are a large class of inorganic oxo clusters that contain early transition metals such as V, Nb, Ta, Mo, and W in their highest oxidation state. They have promising applications in different research domains, including medicine,[23] materials science,[24,25] and catalysis.[26,27] Part of their structure can be removed, resulting in lacunary POM structures that can act as ligands for various metal ions, such as Zn^{2+}, Co^{2+}, and Cu^{2+},[28] which are also found in metalloenzymes. We have previously shown that a number of Zr^{IV}-substituted POM complexes can act as artificial phosphoesterases.[15,21,22] Zr^{IV} is an ideal active center due to its high Lewis acidity and oxophilic properties, which facilitate both the coordination/activation of the substrate/nucleophile and the hydrolysis of the phosphoester bond(s). Among Zr^{IV}-substituted POMs, the mononuclear Zr^{IV}-substituted Wells−Dawson type POM $K_{15}H[Zr(\alpha_2\text{-}P_2W_{17}O_{61})_2]\cdot 25H_2O$ was demonstrated to be able to catalytically enhance the hydrolysis rate of the DNA model compound 4-nitrophenyl phosphate (NPP) by nearly 2 orders of magnitude.[15] In our previous study we also found that the binuclear Zr^{IV}-substituted Keggin type POM $(Et_2NH_2)_8[\{\alpha\text{-}PW_{11}O_{39}Zr(\mu\text{-}OH)(H_2O)\}_2]\cdot 7H_2O$ (ZrK 2:2, Figure 2A) efficiently promoted hydrolysis of the extremely stable DNA model substrate bis-4-nitrophenyl phosphate (BNPP) with a 320-fold rate enhancement[21] and the RNA model substrate 2-hydroxypropyl-4-nitrophenyl phosphate (HPNP) with a 530-fold rate enhancement[29] in comparison to spontaneous hydrolysis.

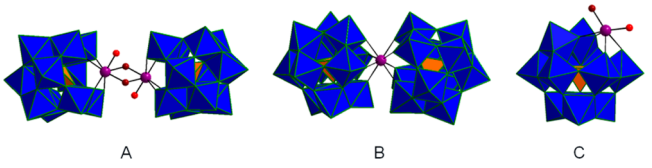

Figure 2. Structures of ZrK 2:2 (A), ZrK 1:2 (B), and ZrK 1:1 (C). The WO_6 groups are represented by blue octahedra, while the internal PO_4 groups are represented by orange tetrahedra. Zr^{IV}, H_2O molecules, and OH groups are represented by violet, red, and dark red balls, respectively.

On the one hand, the aim of the present study is to further explore the reactivity of ZrK 2:2 toward the hydrolysis of phosphoanhydride bonds in the biologically relevant substrate ATP, which has a more complex structure in comparison with previously investigated model DNA substrates (NPP, BNPP). On the other hand, this study aims at fully elucidating the mechanism of this hydrolytic reaction at a molecular level.[21,22] For this purpose we used a combination of ^{31}P, ^{31}P DOSY, and ^{31}P EXSY NMR spectroscopy to monitor the interaction between the POM and the substrate as well as to identify all intermediates formed during the course of the ATP hydrolytic reaction. Diffusion ordered NMR spectroscopy (DOSY) is a powerful technique to study both the presence of the different compounds during the course of complex reactions and interactions at the molecular and supramolecular level. DOSY spectra are two-dimensional maps correlating chemical shifts of the signals along the horizontal dimension and the translational diffusion coefficients of the corresponding species along the vertical dimension. Since the diffusion coefficient reflects the size of the species, different species in complex reaction mixtures can be clearly distinguished on the basis of their diffusion properties, even if their signals overlap along the chemical shift dimension due to their structural similarity. Recently, our research group has successfully applied ^1H and ^{31}P DOSY for the detailed characterization of nanosized organic−inorganic POM-based hybrids[30] and for the study of different POM species present in aqueous solution.[22,31] ^{31}P exchange spectroscopy (EXSY) was applied to reveal the

DOI: 10.1021/acs.inorgchem.6b00385
Inorg. Chem. XXXX, XXX, XXX−XXX

reaction pathways and to gain additional information on the slow dynamic equilibrium between the reaction products and their complexes with the POM. In addition, several comparative experiments were performed to evidence the interaction between ZrK 2:2 and ADP, AMP, P, and PP (Figure 1) formed during ATP hydrolysis. This integrated approach enabled us to propose a detailed reaction mechanism of ATP hydrolysis in the presence of ZrK 2:2.

RESULTS AND DISCUSSION

Interaction between ATP and ZrK 2:2. The aqueous solution speciation of ZrK 2:2 under the reaction conditions used in this study (pD 6.4 and 50 °C) was described in detail in our previous studies and will be only briefly presented here for the purpose of the following discussions.[21,22] Depending on the reaction conditions such as pD, concentration, temperature, and ionic strength, ZrK 2:2 can convert into the less active species $[Zr(PW_{11}O_{39})_2]^{10-}$ (ZrK 1:2, Figure 2B) and/or the more active monomeric Keggin POM species $[\alpha\text{-}PW_{11}O_{39}Zr\text{-}(\mu\text{-}OH)(H_2O)]^{4-}$ (ZrK 1:1, Figure 2C).[21,22] ZrK 1:1 is concluded to be more catalytically active in comparison to ZrK 2:2, as its Zr^{IV} ion has more coordinated water molecules that can be replaced by the substrate or that can act as a nucleophile. Static DFT calculations showed that, depending on pH conditions, the two most stable forms of this monomeric species are the trihydrated form $[\alpha\text{-}PW_{11}O_{39}Zr(H_2O)_3]^{3-}$ and the hydroxomonohydrated form $[\alpha\text{-}PW_{11}O_{39}Zr(\mu\text{-}OH)\text{-}(H_2O)]^{4-}$.[32]

More importantly, in a recent study we have demonstrated that a monomeric Keggin POM species (ZrK 1:1) is present in an aqueous solution of ZrK 2:2 at nearly neutral pD and is responsible for the hydrolysis of the phosphoester bond in BNPP[22] and HPNP.[29] Theoretical studies showed that, when ZrK 1:1 interacts with NPP or BNPP, it forms monodentate complexes which are more stable than the corresponding bidentate complexes.[22] ZrK 1:2 is considered to be less active in comparison to ZrK 2:2 since its Zr atom is coordinatively saturated and hardly accessible for the bulky ATP ligand, as it is sandwiched by the two Keggin moieties. Following our previous findings,[21,22] we consider that the catalytically active POM species responsible for ATP hydrolysis is the monomeric ZrK 1:1 form, which will be abbreviated as ZrK for simplicity.

With the aim of investigating the interaction between ATP and ZrK 2:2, a mixture of 20.0 mM ATP and 3.0 mM ZrK 2:2 at pD 6.4 was incubated at 50 °C. The interaction between ATP and ZrK was evidenced by the characteristic changes observed in ^1H and ^{31}P NMR spectra measured at different time intervals (Figures S1 and S2 in the Supporting Information, respectively). ^1H NMR spectra showed broad overlapping signals of the various species present in the reaction mixture during the course of the ATP hydrolysis and were therefore not useful for a detailed analysis of the reaction mechanism. ^{31}P NMR spectra, however, were much more suitable for this purpose, due to the distinct difference in chemical shifts of the signals. In order to ensure a good signal-to-noise ratio for all signals in ^{31}P spectra, the concentration of ATP was 7 times higher than the concentration of ZrK 2:2. Some representative spectra demonstrating the changes in the ^{31}P spectra of the reaction mixture are shown in Figure 3.

The general reaction mechanism of ATP hydrolysis in the presence of ZrK 2:2 and the expected reaction products and intermediates is presented in Scheme 1. The proposed reaction mechanism is based on careful analysis and full assignment of all signals that appeared and disappeared in ^{31}P spectra during the course of the reaction (Figure S2 in the Supporting Information and Figure 3). We suggest that the reaction can proceed via two parallel pathways, in which the first step is the formation of the two ATP/ZrK complexes I1A (pathway A) and I1B (pathway B).[33] These two ATP/ZrK complexes result from two possible binding modes between ATP and POM. In complex I1A the POM interacts with the terminal phosphate group P_γ of ATP, while in complex I1B the POM binds to the intermediate phosphate group P_β. We suggest that the interaction of the POM and the first phosphate group P_α is not favorable due to the steric repulsion between the bulky POM and the adenosine residue attached to P_α. If the reaction proceeds via pathway A, ATP will be first hydrolyzed to P and ADP, which then can subsequently interact with the POM, forming intermediate I2. In the next step ADP will be further hydrolyzed to AMP and a second P. In contrast, in pathway B, ATP will be hydrolyzed first to AMP and PP. The formation of

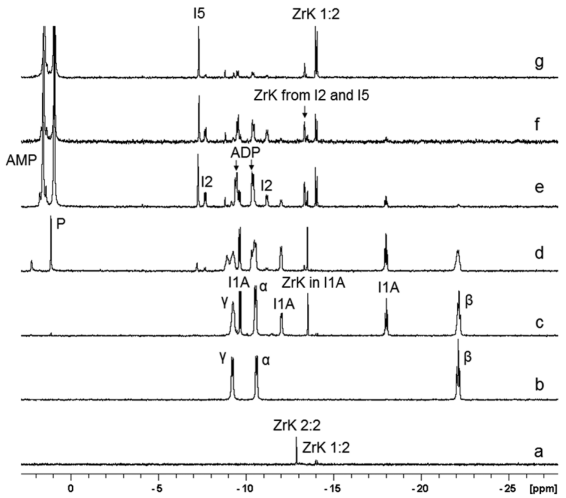

Figure 3. ^{31}P NMR spectra of the hydrolysis reaction: (a) 3.0 mM ZrK 2:2; (b) 20.0 mM ATP; (c–g) 20.0 mM ATP in the presence of 3.0 mM ZrK 2:2 at pD 6.4 measured (c) after pD adjustment and after (d) 3 days, (e) 20 days, (f) 27 days, and (g) 54 days at 50 °C. Conditions: 600 MHz, D_2O, 298 K, NS = 128.

Scheme 1. General Hydrolytic Pattern of ATP in the Presence of ZrK 2:2

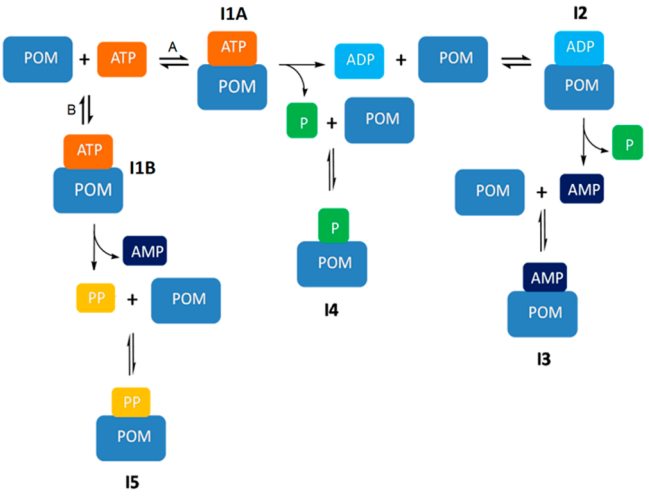

DOI: 10.1021/acs.inorgchem.6b00385
Inorg. Chem. XXXX, XXX, XXX–XXX

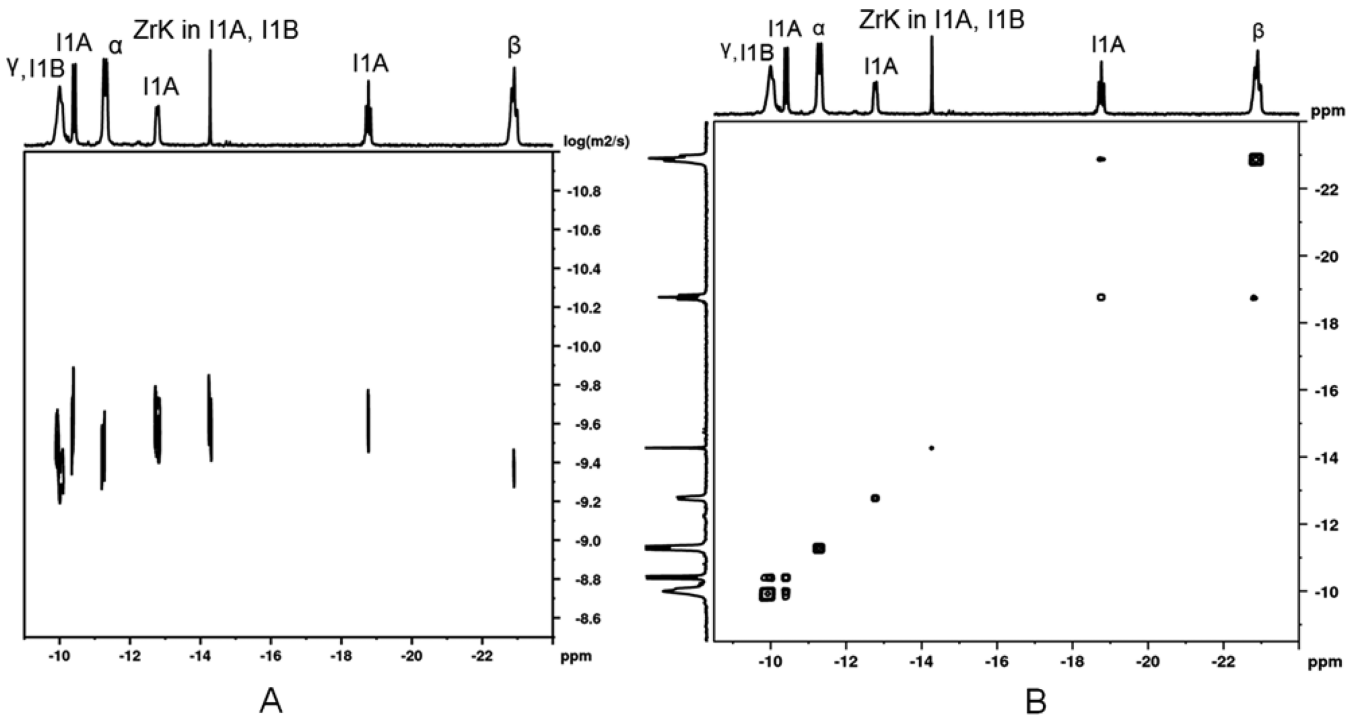

Figure 4. ^{31}P DOSY NMR spectrum (A) and ^{31}P EXSY NMR spectrum (B) of 20.0 mM of ATP in the presence of 3.0 mM of ZrK 2:2 after adjusting to pD 6.4 with no heating.

complexes AMP/ZrK (I3), P/ZrK (I4), and PP/ZrK (I5) was also expected.

Analysis and Signal Assignment of ^{31}P Spectra in Support of the Proposed Reaction Mechanism. Figure 3b shows that the ^{31}P spectrum of a solution of pure ATP at pD 6.4 is characterized by resonances at −9.32 ppm for P_γ, −10.51 ppm for P_α, and −22.08 ppm for P_β. Comparison of the ^{31}P spectra of pure ATP and an ATP/POM mixture measured immediately after pD adjustment without heating (Figure 3c) shows that in the presence of POM small changes in the chemical shifts of all ATP signals (δ −9.23, 10.53, and −22.13 ppm) and a noticeable broadening of the line width of all signals of the free ATP substrate occurs. This broadening (11.97 Hz) is most pronounced for the signal of the terminal phosphate group P_γ. In addition, the appearance of a second set of signals was observed immediately after sample preparation at −9.64, −12.00, and −17.99 ppm, which were assigned to the complex I1A between ATP and POM. We suggest that the complex I1A between the POM and the terminal phosphate group P_γ of the ATP is more stable in comparison to the complex I1B between the POM and the phosphate group P_β in the middle of the phosphate chain of the ATP, which may increase the negative charge on P_β in the transition state[33] and is sterically more hindered. This is why we assume that ATP hydrolysis proceeds mainly through reaction pathway A. The ^{31}P spectra (Figure 3 and Figure S2 in the Supporting Information) show that, during the course of the reaction, the percentage of ATP as well as I1A decreased significantly and the signal of ATP disappeared after 11 days, while the signal of I1A disappeared completely after 20 days.

Figure 3a shows that after pD adjustment ZrK 2:2 (δ −12.89 ppm) partially converts into a small amount of ZrK 1:2 (δ −13.98 and −14.04 ppm).[21] In the presence of 20.0 mM ATP at pD 6.4 the signal of ZrK 2:2 completely shifted to −13.5 ppm.[21] This change in chemical shift of the POM could be a result of the binding to the ATP. Since a high excess of the ATP was used, all POM should be bound to the substrate. Therefore, we proposed that the new peak at −13.5 ppm is the peak of the phosphorus atom from the ZrK bound to ATP in the ATP/ZrK complex (I1A and I1B).

With the aim of confirming the presence of I1A and I1B, we measured the ^{31}P DOSY NMR spectrum of the reaction mixture after sample preparation (Figure 4A). The spectrum shows that there are three main species with different diffusion coefficients. The faster-diffusing species (δ −9.23, −10.53, and −22.13 ppm) with a diffusion coefficient of 4.37×10^{-10} m^2 s^{-1} was assigned to the free unreacted ATP. The diffusion coefficient of the species with a ^{31}P chemical shift of −13.5 ppm was determined to be 2.69×10^{-10} m^2 s^{-1}. The diffusion coefficient measured from the DOSY peaks at the chemical shifts of the new signals that appeared after the addition of the POM and assigned to I1A (δ −9.64, −12.00, and −17.99 ppm) is identical with the diffusion coefficient of the species characterized with a ^{31}P peak at −13.5 ppm. This result indicates that ATP binds to ZrK, since the diffusion of the new species, assigned as an intermediate I1A, is significantly slower than that of ATP.

A careful analysis of the diffusion peak of the broad resonance at −9.23 ppm, assigned to P_γ of the free ATP, showed that this signal has two components along the diffusion dimension (Figure S3 in the Supporting Information). The diffusion coefficient of the first component is identical with those of the free ATP. The second component has a lower diffusion coefficient of 3.24×10^{-10} m^2 s^{-1}, which however is higher in comparison to the diffusion coefficient of the POM. We suggest that this component most probably represents the ATP involved in the less stable intermediate I1B, which exists in a dynamic equilibrium with the free ATP. In this case its apparent diffusion coefficient will be a population-weighted average of the ATP diffusion coefficients in the bound and free

DOI: 10.1021/acs.inorgchem.6b00385
Inorg. Chem. XXXX, XXX, XXX−XXX

states. This suggestion also explains the observed broadening of the ATP signals upon addition of the POM resulting from the exchange process and the partial overlap of the ATP and I1B resonances. Figure S3 shows the expanded areas of the spectrum of the reaction mixture, where the presence of additional low-intensity signals partially overlapping with the main ATP resonances is clearly seen. The relatively high value of the diffusion coefficient of I1B and the very small chemical shift differences of the signals of free ATP and I1B complex indicate that the equilibrium is shifted toward the free ATP due to the low stability of intermediate I1B.

The presence of a dynamic equilibrium between ATP and the intermediates I1A and I1B was further investigated by ^{31}P EXSY NMR. Figure 4B shows the ^{31}P EXSY spectrum of a mixture of 20.0 mM of ATP and 3.0 mM of ZrK 2:2, where the exchange cross-peaks originating from a slow exchange between ATP and the more stable intermediate I1A are clearly seen. Due to the partial overlap of ATP and I1B signals the cross-peaks between these species are not detectable.

After incubation of the sample for 3 days at 50 °C, the appearance of new signals in addition to those of ATP and I1 was detected (Figure 3d). The singlets at 2.24 and 1.14 ppm were assigned to the reaction products AMP and P, respectively, while the two broad doublets at −9.26 and −10.36 ppm, which are partially overlapped with the signals of P_γ and P_α of the unreacted ATP, were assigned to ADP by comparison with the ^{31}P spectra of pure AMP, P, and ADP (Figures S4−S6 in the Supporting Information). The broad resonance at around −8.94 ppm originates from free PP formed as a reaction product following pathway B, while the low-intensity signal at around −7.25 ppm was assigned to I5, representing the complex between the ZrK and the PP, as demonstrated by comparison with the reference spectra of pure PP and of PP in the presence of ZrK 2:2 (Figure S7 in the Supporting Information). In addition, two doublets with very low intensity at −7.65 and −11.20 ppm were also observed. We suggest that these signals originate from intermediate I2, representing a complex between ADP and ZrK. The ^{31}P DOSY NMR spectrum in Figure 5 provides further evidence for the appearance of AMP, P, and I5. We can see from Figure 5 that P is the smallest species, represented by the highest diffusion coefficient of 7.59×10^{-10} m^2 s^{-1}. The second species with the diffusion coefficient of 4.67×10^{-10} m^2 s^{-1} was assigned as AMP. The diffusion coefficient measured at the chemical shift of the signal assigned to I5 (2.67×10^{-10} m^2 s^{-1}) is similar to the diffusion coefficient of the ZrK and the I1A, thus confirming that this resonance originates from the complex between PP and ZrK. Due to the much larger molecular weight of the POM the diffusion coefficients of all intermediates are dominated by the POM diffusion coefficient. Unfortunately, due to partial overlap of the ADP signals with the resonances of P_γ and P_α of the nonreacted ATP, a precise determination of the ADP diffusion coefficient in this reaction mixture is hampered. The simultaneous presence of ADP, AMP, P, and PP in the reaction mixture indicates that the two pathways shown in Scheme 1 for the hydrolysis of ATP in the presence of ZrK 2:2 proceed in parallel.

With the advancement of the reaction after heating for 20 days at 50 °C (Figure 3e), the signals of ATP almost disappear, while the intensity of I1A resonances significantly decreased. In parallel to that, the intensity of the resonances assigned to ADP, PP, AMP, and P as well as I5 and I2 complexes increased (Figure 3e). The appearance of a new set of signals at −13.98

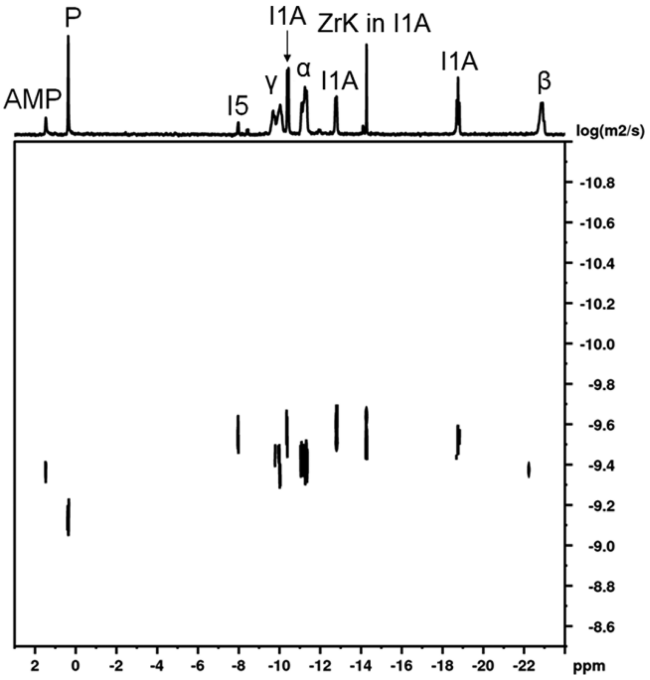

Figure 5. ^{31}P DOSY NMR spectrum of 20.0 mM of ATP in the presence of 3.0 mM of ZrK 2:2 after 3 days at 6.4 and 50 °C.

and −14.04 ppm characteristic for ZrK 1:2 showed that at this stage of the reaction ZrK 2:2 has partially converted into its less reactive form.

After incubation of the reaction mixture for 27 days at 50 °C, ATP and I1 completely disappeared and their signals were no longer observed in the ^{31}P spectrum (Figure 3f). At this stage of the reaction the two doublets at −9.26 and −10.36 ppm assigned to free ADP as well as the pair of doublets of the intermediate I2 between ADP and ZrK at −7.65 and −11.20 ppm were clearly seen. The longer incubation time resulted also in an increase in the amount of I5 (the complex between PP and ZrK) in the reaction mixture, as evidenced by the higher intensity of the signal at −7.25 ppm in comparison to its intensity after 3 days of heating at 50 °C (Figure 3d). During the course of the reaction the intensity of ADP increased, reaching a maximum after 7 days, and then gradually decreased (Figure 3 and Figure S2 in the Supporting Information). The disappearance of ATP and I1 and the higher signal intensity of ADP and I2 at this stage of the reaction allowed better resolution and sensitivity in the ^{31}P DOSY spectrum of the reaction mixture (Figure 6), which gave further evidence for the formation of ADP and I2. The results show that the diffusion coefficient (2.75×10^{-10} m^2 s^{-1}) of the species at δ −7.65 and −11.20 ppm assigned as I2 is lower than that (4.63×10^{-10} m^2 s^{-1}) of the species at δ −9.26 and −10.36 ppm assigned as ADP. The data are in full agreement with the chemical shifts and diffusion coefficients determined in a comparative study of a mixture of 20.0 mM ADP and 3.0 mM ZrK 2:2 (Figure S6 in the Supporting Information). The chemical shifts and the diffusion coefficients of the various species observed during the course of the reaction are summarized in Table 1.

The slow exchange between ADP and I2 in this reaction mixture was observed by ^{31}P EXSY NMR. Figure 7 shows the expanded ^{31}P EXSY spectrum in the region from −6 to −15 ppm, where the exchange cross-peaks between ADP and I2 are clearly seen. The full ^{31}P EXSY NMR spectra of the reaction

DOI: 10.1021/acs.inorgchem.6b00385
Inorg. Chem. XXXX, XXX, XXX−XXX

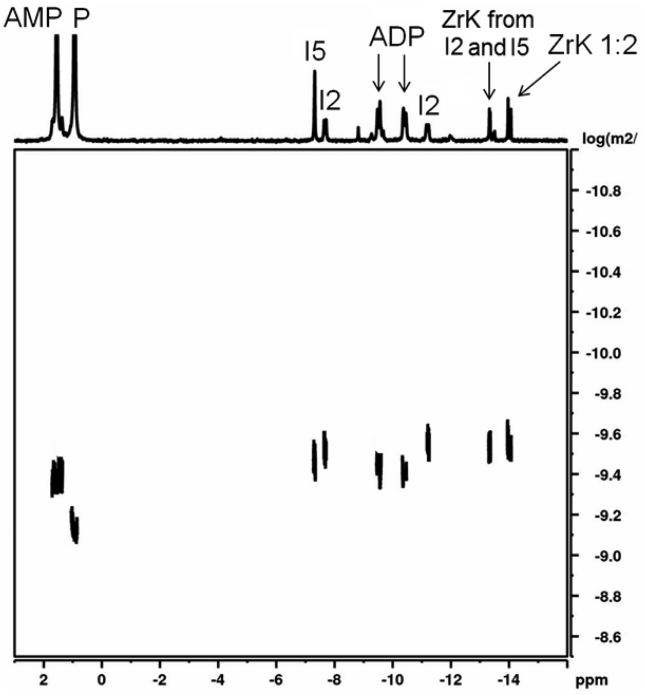

Figure 6. ^{31}P DOSY NMR spectrum of 20.0 mM of ATP in the presence of 3.0 mM of ZrK 2:2 after 27 days at pD 6.4 and 50 °C.

Table 1. Chemical Shifts and Diffusion Coefficients of the Various Species Observed during ATP Hydrolysis in the Presence of ZrK 2:2

species	chem shift (ppm)	diffusion coeff (m^2 s^{-1})
ATP	−9.23, −10.53, −22.13	4.37×10^{-10} ($\pm 5.82 \times 10^{-13}$)
I1A	−9.64, −12.00, −17.99	2.69×10^{-10} ($\pm 2.78 \times 10^{-12}$)
I1B	−9.23	3.24×10^{-10} ($\pm 3.87 \times 10^{-12}$)
ADP	−9.26, −10.36	4.63×10^{-10} ($\pm 7.49 \times 10^{-13}$)
I2	−7.65, −11.20	2.75×10^{-10} ($\pm 4.25 \times 10^{-12}$)
AMP	2.24	4.67×10^{-10} ($\pm 3.87 \times 10^{-13}$)
P	1.14	7.59×10^{-10} ($\pm 1.23 \times 10^{-13}$)
I5	−7.25	2.67×10^{-10} ($\pm 8.56 \times 10^{-12}$)
ZrK 1:1	−13.5	2.69×10^{-10} ($\pm 6.33 \times 10^{-12}$)

mixture measured after heating at 50 °C for 20 and 27 days, respectively, are given in Figures S8 and S9 in the Supporting Information. Both spectra have similar cross-peak patterns.

Figure S2 in the Supporting Information shows that upon further incubation at 50 °C the signals of ADP and I2 gradually decreased and disappeared after 54 days (Figure 3g). In parallel to that, the intensity of P and AMP signals increased during the course of the reaction. After 54 days the only components present in the mixture are the reaction products P and AMP as well as I5. Upon further heating the intensity of I5 slowly decreased, indicating that I5 slowly converted into P. The slow conversion of I5 to P can be explained by the fact that the PP linkage in I5 is probably stabilized by the Zr^{IV} ion of ZrK.[34]

The analysis of ^{31}P spectra in Figure 3 showed that no signals indicative of the presence of I3 and I4 intermediates could be found. We suggest that, since AMP is an unactivated phosphate

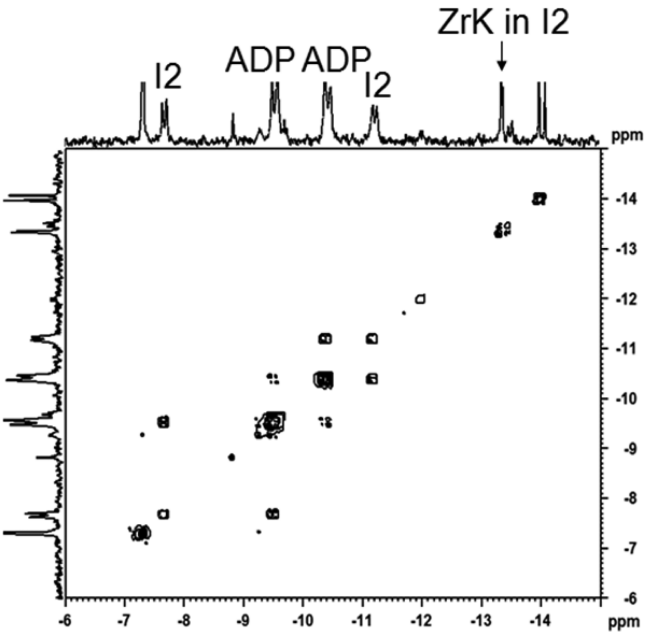

Figure 7. ^{31}P EXSY NMR spectrum of 20.0 mM ATP in the presence of 3.0 mM ZrK 2:2 after 27 days at pD 6.4 and 50 °C.

monoester due to the absence of an leaving group such as *p*-nitrophenyl, it is much more resistant to hydrolysis.[35] With the aim of providing more information about the interaction between AMP and ZrK 2:2, we recorded ^{31}P NMR spectra of a mixture of 20.0 mM AMP and 3.0 mM ZrK 2:2 in D_2O at pD 6.4 after pD adjustment and after different time increments at 50 °C (Figure S4 in the Supporting Information). The results show that immediately after mixing three new resonances appeared at −2.79, −13.20, and −13.28 ppm. We suggest that the new resonances originate from a complex between AMP and ZrK (I3). We suggest that the peak at −2.79 ppm and one of the two peaks at around −13 ppm originate from the AMP/ZrK complex I3, while the other peak at around −13 ppm is eventually from the free ZrK. The intensity of these signals gradually decreased when the incubation time increased, and they completely disappear after 6 days at 50 °C, suggesting that complex I3 was not stable and disintegrates back to AMP and ZrK, which further converts to ZrK 1:2, as evidenced by the two characteristic new peaks at −13.98 and −14.04 ppm. Unfortunately, due to the very low intensity of I3 and ZrK it was not possible to measure ^{31}P DOSY and ^{31}P EXSY spectra of this mixture. In addition to the observed new signals in the presence of 3.0 mM of ZrK 2:2 the peak of the free AMP was shifted upfield by 0.20 ppm and its half-width increased to 17.32 Hz. Both the change in chemical shift and the line broadening of the signal of the free AMP indicated that it is involved in dynamic equilibrium with the I3 complex. In a high excess of the AMP substrate this equilibrium is shifted toward the free AMP, as evidenced by the disappearance of the resonances of I3 after 6 days. After 6 days of heating at 50 °C, the signal of AMP was still very stable, suggesting that AMP was not hydrolyzed.

Similarly, the potential formation of the complex I4 between P and ZrK was confirmed by comparative studies of a mixture of 20.0 mM Na_2HPO_4 and 3.0 mM ZrK 2:2 (Figure S5 in the Supporting Information). In addition to the resonances of free phosphate (1.14 ppm) and ZrK 2:2 (−12.89 ppm), the ^{31}P spectrum of this mixture shows two weak signals at −2.32 and

DOI: 10.1021/acs.inorgchem.6b00385
Inorg. Chem. XXXX, XXX, XXX−XXX

−13.28 ppm (Figure S5b). We suggest that these signals originate from the I4 complex and correspond to the phosphorus atom of the phosphate (−2.32 ppm) and of the ZrK (−13.28 ppm) involved in the I4 complex. These signals completely disappear after 4 days at 50 °C, suggesting that similarly to I3 this complex is not very stable and in excess Na_2HPO_4 it disintegrates to P and ZrK 1:2, as evidenced by the two characteristic new peaks at −13.98 and −14.04 ppm (Figure S5c). These results are in agreement with the observations in the comparative study of a 20.0 mM AMP and 3.0 mM ZrK 2:2 reaction mixture, where the excess AMP favored the release of free substrate from I3. To further assess the influence of sample composition on the stability of I4, we investigated an equimolar mixture of 6.0 mM Na_2HPO_4 and 6.0 mM ZrK 2:2. The ^{31}P spectrum (Figure S5d) shows that in this case the equilibrium is shifted toward the I4 complex, as evidenced by a higher intensity of I4 signals in comparison to the signals of free P and ZrK 2:2.

The observations based on the comparative studies of AMP/ZrK 2:2 and Na_2HPO_4/ZrK 2:2 mixtures described above could explain why I3 and I4 were not observed during the ATP hydrolysis, as evidenced by the lack of signals at −2.79 ppm (I3) and −2.32 ppm (I4) in the ^{31}P spectra of the 20.0 mM ATP and 3.0 mM ZrK 2:2 reaction mixture (Figure 3). Under the reaction conditions their analytical concentration is very low, since they quickly convert to AMP and P, as demonstrated by the comparative studies of AMP/ZrK 2:2 and Na_2HPO_4/ZrK 2:2 mixtures.

The percentage of each species formed during the ATP hydrolysis in the presence of ZrK 2:2 was determined by integration of its respective ^{31}P signal(s) and plotted as a function of reaction time (Figure 8).

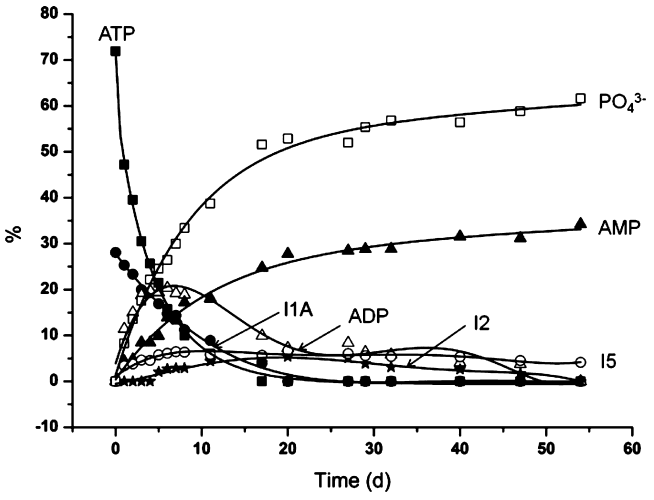

Figure 8. Percentage of all species (ATP, I1A, ADP, I2, I5, AMP, and P) formed during the course of the reaction as a function of reaction time for the reaction between 20.0 mM of ATP and 3.0 mM of ZrK 2:2 at pD 6.4 and 50 °C.

Proposed Mechanism. On the basis of the above results, a detailed mechanism of ATP hydrolysis in the presence of ZrK 2:2 is proposed in Scheme 2.[21,22,29] As mentioned above under these reaction conditions, there is an equilibrium among ZrK 2:2, ZrK 1:1, and/or ZrK 1:2. ATP coordination to ZrK 1:2 is not expected, since the Zr atom in ZrK 1:2 is coordinatively saturated and hardly accessible to the bulky ATP ligand. ZrK 1:1 is more catalytically active in comparison to ZrK 2:2, since its Zr^{IV} ion has more coordinated water molecules that can be replaced by the substrate or that can act as a nucleophile. Therefore, we proposed that in this study ZrK 1:1 is also the most active species and it is responsible for substrate phosphoanhydride bond hydrolysis. When ATP is added to a ZrK 2:2 solution under the same reaction conditions, ZrK 1:1 coordinates to the oxygen atom of a terminal and intermediate phosphate group of ATP, forming intermediates I1A and I1B, respectively. The coordination of ZrK 1:1 to P_γ is favored, since it is suggested to have the catalytic function of stabilizing the development of negative charge on the γ-phosphoryl oxygen of ATP.[33,36] This coordination results in more positive charge at the P_γ atom, thus activating it toward nucleophilic attack. In I1A the OH group or the coordinated water of ZrK 1:1 can play the role of a nucleophile, attacking the phosphorus atom and leading to P−O bond cleavage and formation of I4 and ADP following pathway A. In the next reaction step along this pathway ADP binds to ZrK 1:1 in a similar way, forming intermediate I2. The intramolecular attack of the OH group of ZrK 1:1 to the phosphorus atom also leads to P−O bond cleavage, resulting in the reaction products AMP and P. The parallel hydrolytic pathway B also occurs, where ZrK 1:1 interacts with the P_β phosphorus atom of ATP in an identical way, forming the intermediate I1B and then leading to the formation of I5 and AMP. The formation of intermediates I3 and I4 is also possible; however, they are not stable under the reaction conditions since the excess of AMP and P, whose concentration constantly increases during the reaction, favors their conversion back to AMP and P.

In general ZrK 1:1 can bind to the phosphate group of the ATP substrate in a mono- or bidentate fashion. In our prevoius study on the phosphoester bond hydrolysis in BNNP, promoted by ZrK 2:2, we demostrated by DFT calculations that the monodentate BNPP/ZrK 1:1 complex is more favorable.[22] The hydrolysis of the first phosphoester bond in BNPP results in the formation of NPP, which further interacts with ZrK 1:1. ^{31}P EXSY NMR spectra showed that the bidentate NPP/POM complex exists in a dynamic equilibrium with the monobound and free NPP. We suggest that ATP interacts with ZrK 1:1 in an identical way, resulting in both mono- and bidentate coordination of the substrate to ZrK 1:1. Unfortunately in this case the NMR data do not give sufficient evidence to fully elucidate the type of the binding mode, since apart from the broad resonance at −9.23 ppm for the I1B which is however overlapped by the signal of P_γ of the free ATP, we obseved only one set of NMR signals for the other phosphorus atoms from the phosphoester chain in both bound species. The reason could be the fast interconversion between the two types of coordination modes with respect to the NMR chemical shift time scale, resulting in one averaged set of resonances.

During the course of ATP hydrolysis, no signal of triphosphate (PPP, Figure 1) is detected, meaning that ATP cannot be immediately hydrolyzed at P_α to PPP, most probably due to the steric hindrance of the adenosine residue attached to P_α.

The proposed complex reaction mechanism of ATP hydrolysis in the presence of ZrK 2:2 was further supported by a comparative study of the interaction of ZrK 2:2 with ADP, AMP, PP, and P used as substrates. This strategy facilitated the analysis of the otherwise complex spectral patterns of ATP/ZrK mixtures and allowed us to unequivocally assign all the reaction

DOI: 10.1021/acs.inorgchem.6b00385
Inorg. Chem. XXXX, XXX, XXX−XXX

Scheme 2. Proposed Reaction Mechanism for the Hydrolysis of ATP by ZrK 2:2[a]

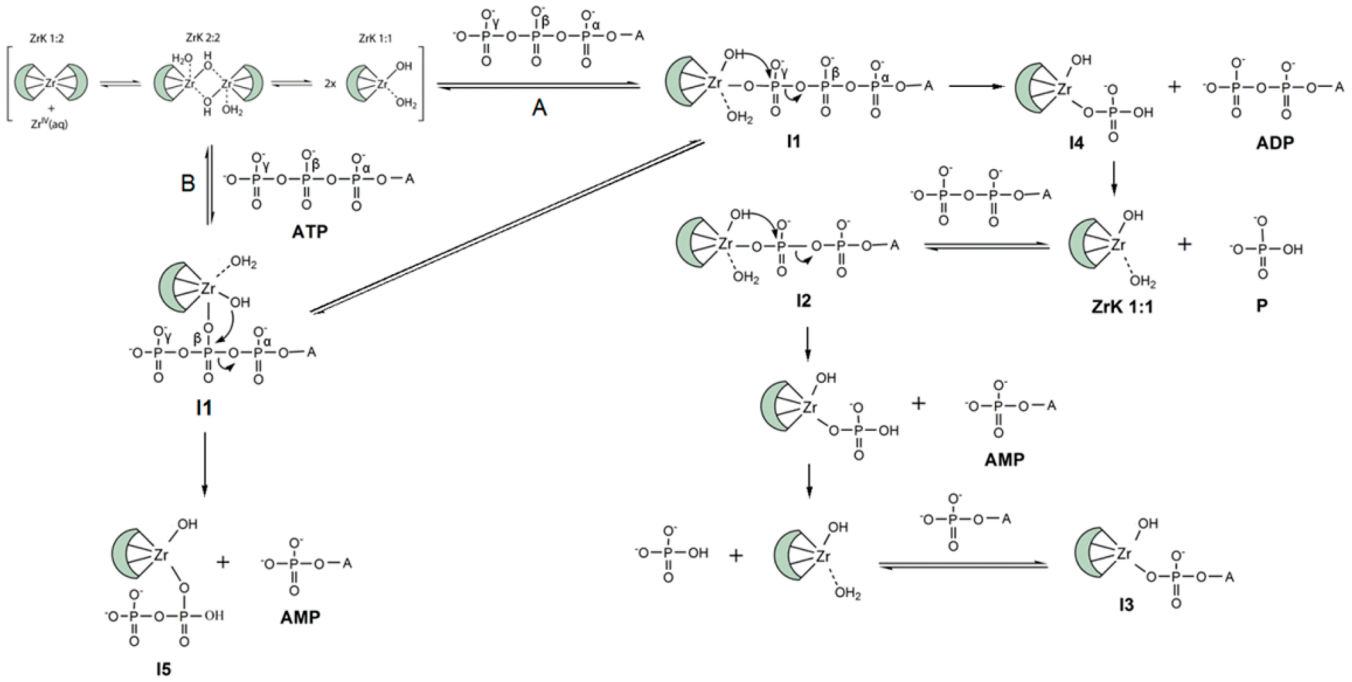

[a]In this scheme, A in all compounds represents a ribose sugar and a nucleoside base adenosine part.

products and intermediates. The chemical shift fingerprint of the new species observed during the hydrolysis of ATP with those identified in the comparative reaction mixtures confirmed that the reaction proceeds through the proposed reaction steps and pathways. The ^{31}P spectra of the comparative mixtures are presented and described in detail in Figures S4–S7 and S10–S12 in the Supporting Information.

Kinetic Study. The full assignment of all species that occur during the course of ATP hydrolysis in the presence of ZrK 2:2 facilitated a kinetic study. In order to evaluate the reactivity of ZrK 2:2 toward ATP hydrolysis, the observed rate constants of ATP (20.0 mM) hydrolysis in the presence of 3.0 mM ZrK 2:2 at pD 6.4 and 50 °C were determined. Since the hydrolysis of ATP in the presence of ZrK 2:2 is complicated due to the formation of several intermediates and products, the calculation of the rate constant of the hydrolysis was simplified by focusing on the disappearance of both ATP and stable intermediate I1A signals. The first-order rate constants were calculated from the simple expression $-d[\mathrm{ATP}]_t/dt = k_{obs}[\mathrm{ATP}]_t$, where $[\mathrm{ATP}]_t$ represents the total concentration of all forms of ATP, including nonreacted ATP and ATP, in the intermediate (I1A).[17] Integration of the ATP and I1A ^{31}P NMR spectroscopic resonances (Figure S2 in the Supporting Information and Figure 8) at different time increments allowed the calculation of the ATP hydrolysis rate constant. A linear fitting method ($\ln[\mathrm{ATP}] = k_{obs}t + \ln[\mathrm{ATP}]_0$; Figure S13 in the Supporting Information), where $[\mathrm{ATP}] = [\mathrm{ATP}]_{nonreacted} + [\mathrm{I1}]$ is the concentration of the ATP at time t, was used. The hydrolysis rate constant for ATP hydrolysis was calculated to be $(1.97 \pm 0.17) \times 10^{-6}$ s^{-1} at pD 6.4 and 50 °C. We expected the rate constant of ATP hydrolysis promoted by the Zr^{4+} salt $ZrCl_2O{\cdot}8H_2O$ to be slower than that promoted by ZrK 2:2. Unfortunately, a comparison of these rate constants was impossible because the activity of Zr^{4+} in the absence of ligands could not be determined due to the formation of precipitates.[37] However, our previous study showed that, under the same conditions (pD 6.4 and 50 °C), the rate constant of HPNP hydrolysis promoted by $ZrCl_2O{\cdot}8H_2O$ is 40-fold slower than that promoted by ZrK 2:2 due to the formation of insoluble Zr^{IV} hydroxyl polymeric gels.[29]

To observe the influence of catalyst concentration on the observed rate constant, as well as its influence on the different intermediates formed in the course of hydrolytic reaction, the rate constant of 3.0 mM ATP hydrolysis was measured in the presence of 3.0 mM ZrK 2:2 at pD 6.4 and 50 °C. ^{31}P NMR spectra were recorded at different time intervals (Figure S14 in the Supporting Information). As can be seen from Figure S14, under these conditions no free ATP resonances were seen, but the resonances of I1 (−9.64, −12.00, −17.99 ppm) were clearly detected, suggesting that ATP completely converted into I1A. In addition, the signal of free ZrK 2:2 at −12.89 ppm and of ZrK at −13.5 ppm appeared simultaneously after pD adjustment. Integration of the I1 ^{31}P resonances at different time increments allowed the calculation of the ATP hydrolysis rate constant. A linear fitting method ($\ln[\mathrm{ATP}] = k_{obs}t + \ln[\mathrm{ATP}]_0$) (Figure S15 in the Supporting Information), where $[\mathrm{ATP}] = [\mathrm{I1}]$ is the concentration of the ATP at time t, was used and the rate constant for ATP hydrolysis was calculated to be $(1.04 \pm 0.11) \times 10^{-5}$ s^{-1}.

The results from the kinetic experiments imply that the relative ratio of the substrate and the POM influences the rate of the ATP hydrolysis and the type of intermediates formed during the course of the reaction. This finding is important in view of the eventual practical applications of POMs as artificial phosphatases, since it demonstrates that it is possible to control the reaction rate by careful tuning of sample composition.

CONCLUSION

In this study we have proposed a detailed mechanism for ATP hydrolysis in the presence of ZrK 2:2 elucidated by ^{31}P, ^{31}P DOSY, and ^{31}P EXSY NMR spectroscopy. The results clearly

DOI: 10.1021/acs.inorgchem.6b00385
Inorg. Chem. XXXX, XXX, XXX−XXX

demonstrate that ^{31}P DOSY NMR is a powerful technique to determine in situ the presence of reaction intermediates (I1A, I1B, I2, and I5) and products (ADP, AMP, P) formed during the course of ATP hydrolysis. In addition, ^{31}P EXSY NMR has been proven to be a very useful technique to identify the presence of slow exchange between the intermediates and the reaction products (ATP, I1A and I1B; ADP, I2; PP, I5) and to follow the reaction pathway. The assignment of all species that occurred during ATP hydrolysis promoted by this POM allowed calculation of the rate constants. The present study further demonstrates the potential of Zr^{IV}-substituted POMs as artificial phosphatases[15,21,22,29] and contributes to the further development of POMs as Lewis acid catalysts for the hydrolysis of biomolecules.[38−40] Understanding the detailed mechanism in this study encourages us to further exploit the hydrolytic activity of this POM toward biologically active molecules such as DNA/RNA fragments, pesticides (paraoxon, parathion), and nerve agents (soman, sarin).

EXPERIMENTAL SECTION

Materials. The binuclear Zr^{IV}-substituted Keggin POMs $(Et_2NH_2)_8[\{\alpha\text{-}PW_{11}O_{39}Zr(\mu\text{-}OH)(H_2O)\}_2]\cdot 7H_2O$[41,42] (ZrK 2:2) and $(Et_2NH_2)_{10}[Zr(PW_{11}O_{39})_2]\cdot 7H_2O$ (ZrK 1:2)[43] were synthesized as described in the literature. Adenosine triphosphate (ATP), adenosine diphosphate (ADP), adenosine monophosphate (AMP), sodium pyrophosphate (PP), Na_2HPO_4 (P), ribose phosphate, adenine, adenosine, DCl, and NaOD were purchased from Acros and used without any further purification.

Sample Preparation. Solutions containing 20.0 mM of each compound ATP, ADP, AMP, PP, and Na_2HPO_4 and 3.0 mM of ZrK 2:2 were prepared in D_2O for the interaction study. An additional solution containing 3.0 mM ATP and 3.0 mM ZrK 2:2 was prepared in D_2O for the kinetic study. The final pD of the solution was adjusted with minor amounts of concentrated DCl (10%) and NaOD (15%). The pH meter value was corrected by using the equation: pD = (pH meter reading) + 0.41.[44]

NMR Measurements. ^{31}P 1D NMR spectra were recorded on a Bruker Avance 400 spectrometer. Trimethyl phosphate was used as the ^{31}P chemical shift external reference. The ^{31}P DOSY and EXSY spectra were measured on a Bruker Avance II+ 600 NMR spectrometer using a 5 mm direct detection dual broad band probe, with a gradient coil delivering a maximum gradient strength of 53 G/cm. All experiments were performed at a temperature of 298 K. The 2D EXSY spectra were recorded with the Bruker program *noesygpph*. The spectra were recorded with a spectral width of 25000 Hz, 2 K data points in the t2 time domain and 256 t1 increments with 64 transients each, and a relaxation delay of 3 s. The spectra were recorded for each sample with two different mixing times of 300 and 400 ms. A sine window function (ssb = 2) and zero-filling were applied in both dimensions prior to Fourier transformation, to give a 4K × 4K data matrix in the frequency domain. The ^{31}P DOSY spectra were measured using a stimulated echo based pulse sequence, with bipolar sine shaped gradient pulses. The spectra were acquired with 64K time domain data points in the t2 dimension, 32 gradient strength increments, a diffusion delay of 200 ms, a total gradient pulse length of 7 ms, 128 transients for each gradient step, and a relaxation delay of 6 ms. The gradient strength was incremented from 2 to 80% of the maximum gradient output (from 0.68 to 27.25 G/cm). The spectra were processed with an exponential window function (line broadening factor 5), 64K data points in F2, and 258 data points in the diffusion dimension. The evaluation of the diffusion coefficients was performed by fitting the diffusion profile (the normalized signal intensity as a function of the gradient strength G) at the chemical shift of each signal in the DOSY spectrum with an exponential function using a variant of the Stejskal−Tanner equation adapted to the particular pulse sequence used.

ASSOCIATED CONTENT

Supporting Information

The Supporting Information is available free of charge on the ACS Publications website at DOI: 10.1021/acs.inorgchem.6b00385.

^{31}P, ^{31}P DOSY, and ^{31}P EXSY NMR spectra, the interaction between ADP/AMP/P/PP and ZrK 2:2, the interaction between the substrates structurally related to ATP and ZrK 2:2, and ln[ATP] as a function of time (PDF)

AUTHOR INFORMATION

Corresponding Authors

*P.S.: e-mail, psd@orgchm.bas.bg.

*T.N.P.-V.: e-mail, tatjana.vogt@chem.kuleuven.be; web, www.chem.kuleuven.be/lbc/.

Author Contributions

The manuscript was written through contributions of all authors. All authors have given approval to the final version of the manuscript.

Notes

The authors declare no competing financial interest.

ACKNOWLEDGMENTS

T.N.P.-V. and P.S. (BOF + fellowship) thank KU Leuven for financial support. T.K.N.L. thanks the Vietnamese Government and KU Leuven for a doctoral fellowship. G.A. thanks FWO Flanders for a postdoctoral fellowship. The authors acknowledge the CMST COST Action CM1203 (Polyoxometalate Chemistry for Molecular Nanoscience) for financial support in terms of STSM applications.

REFERENCES

(1) Bazzicalupi, C.; Bencini, A.; Bianchi, A.; Danesi, A.; Giorgi, C.; Lodeiro, C.; Pina, F.; Santarelli, S.; Valtancoli, B. *Chem. Commun.* **2005**, 2630.

(2) Massoud, S. S.; Milburn, R. M. *J. Inorg. Biochem.* **1990**, *39*, 337.

(3) Guo, Y.; Ge, Q.; Lin, H.; Lin, H. K.; Zhu, S.; Zhou, C. *Biophys. Chem.* **2003**, *105*, 119.

(4) Fidelis Manyanga, A. S.; Science Math Zone, Inc.: Boston, 2014.

(5) Edmunds, T.; Goldberg, A. L. *J. Cell. Biochem.* **1986**, *32*, 187.

(6) Ge, R.; Lin, H.; Xu, X.; Sun, X.; Lin, H.; Zhu, S.; Ji, B.; Li, F.; Wu, H. *J. Inorg. Biochem.* **2004**, *98*, 917.

(7) Imamura, T.; Hinton, D. M.; Belford, R. L.; Gumport, R. I.; Haight, G. P., Jr *J. Inorg. Biochem.* **1979**, *11*, 241.

(8) Millán, J. L. *Purinergic Signalling* **2006**, *2*, 335.

(9) Nayudu, R. V.; de Meis, L. *FEBS Lett.* **1989**, *255*, 163.

(10) Spencer, A. G. University of London, Athlone Press: 1964.

(11) Hegg, E. L.; Burstyn, J. N. *Coord. Chem. Rev.* **1998**, *173*, 133.

(12) Kitamura, Y.; Komiyama, M. *Nucleic Acids Res.* **2002**, *30*, 102e.

(13) Fang, Y.-G.; Zhang, J.; Chen, S.-Y.; Jiang, N.; Lin, H.-H.; Zhang, Y.; Yu, X.-Q. *Bioorg. Med. Chem.* **2007**, *15*, 696.

(14) Thomas, D. T. In *Metal-DNA Chemistry*; American Chemical Society: Washington, DC, 1989; Vol. *402*, p 1.

(15) Vanhaecht, S.; Absillis, G.; Parac-Vogt, T. N. *Dalton Transactions* **2012**, *41*, 10028.

(16) Schneider, P. W.; Brintzinger, H. *Helv. Chim. Acta* **1964**, *47*, 1717.

(17) Hediger, M.; Milburn, R. M. *J. Inorg. Biochem.* **1982**, *16*, 165.

(18) Wilcox, D. E. *Chem. Rev.* **1996**, *96*, 2435.

(19) Sträter, N.; Lipscomb, W. N.; Klabunde, T.; Krebs, B. *Angew. Chem., Int. Ed. Engl.* **1996**, *35*, 2024.

(20) Absillis, G.; Cartuyvels, E.; Van Deun, R.; Parac-Vogt, T. N. *J. Am. Chem. Soc.* **2008**, *130*, 17400.

DOI: 10.1021/acs.inorgchem.6b00385
Inorg. Chem. XXXX, XXX, XXX−XXX

(21) Luong, T. K. N.; Absillis, G.; Shestakova, P.; Parac-Vogt, T. N. *Eur. J. Inorg. Chem.* **2014**, *2014*, 5276.
(22) Luong, T. K. N.; Shestakova, P.; Mihaylov, T. T.; Absillis, G.; Pierloot, K.; Parac-Vogt, T. N. *Chem. - Eur. J.* **2015**, *21*, 4428.
(23) Stephan, H.; Kubeil, M.; Emmerling, F.; Müller, C. E. *Eur. J. Inorg. Chem.* **2013**, *2013*, 1585.
(24) Carraro, M.; Gross, S. *Materials* **2014**, *7*, 3956.
(25) Proust, A.; Matt, B.; Villanneau, R.; Guillemot, G.; Gouzerh, P.; Izzet, G. *Chem. Soc. Rev.* **2012**, *41*, 7605.
(26) Izarova, N. V.; Pope, M. T.; Kortz, U. *Angew. Chem., Int. Ed.* **2012**, *51*, 9492.
(27) Sartorel, A.; Bonchio, M.; Campagna, S.; Scandola, F. *Chem. Soc. Rev.* **2013**, *42*, 2262.
(28) Sigel, H.; Marcel Dekker: New York, 1983; Vol. *15*.
(29) Luong, T. K. N.; Absillis, G.; Shestakova, P.; Parac-Vogt, T. N. *Dalton Transactions* **2015**, *44*, 15690.
(30) Shestakova, P.; Absillis, G.; Martin-Martinez, F. J.; De Proft, F.; Willem, R.; Parac-Vogt, T. N. *Chem. - Eur. J.* **2014**, *20*, 5258.
(31) Stroobants, K.; Absillis, G.; Shestakova, P.; Willem, R.; Parac-Vogt, T. *J. Cluster Sci.* **2014**, *25*, 855.
(32) Jiménez-Lozano, P.; Carbó, J. J.; Chaumont, A.; Poblet, J. M.; Rodríguez-Fortea, A.; Wipff, G. *Inorg. Chem.* **2014**, *53*, 778.
(33) Admiraal, S. J.; Herschlag, D. *Chem. Biol.* **1995**, *2*, 729.
(34) Rainey, J. M.; Jones, M. M.; Lockhart, W. L. *J. Inorg. Nucl. Chem.* **1964**, *26*, 1415.
(35) Chin, J.; Banaszczyk, M. *J. Am. Chem. Soc.* **1989**, *111*, 4103.
(36) Williams, N. H. *J. Am. Chem. Soc.* **2000**, *122*, 12023.
(37) Jagoda, M.; Krämer, R. *Inorg. Chem. Commun.* **2005**, *8*, 697.
(38) Stroobants, K.; Absillis, G.; Moelants, E.; Proost, P.; Parac-Vogt, T. N. *Chem. - Eur. J.* **2014**, *20*, 3894.
(39) Stroobants, K.; Goovaerts, V.; Absillis, G.; Bruylants, G.; Moelants, E.; Proost, P.; Parac-Vogt, T. N. *Chem. - Eur. J.* **2014**, *20*, 9567.
(40) Ly, H. G. T.; Absillis, G.; Janssens, R.; Proost, P.; Parac-Vogt, T. N. *Angew. Chem., Int. Ed.* **2015**, *54*, 7391.
(41) Nomiya, K.; Saku, Y.; Yamada, S.; Takahashi, W.; Sekiya, H.; Shinohara, A.; Ishimaru, M.; Sakai, Y. *Dalton Transactions* **2009**, 5504.
(42) Ly, H. G. T.; Absillis, G.; Parac-Vogt, T. N. *Dalton Transactions* **2013**, *42*, 10929.
(43) Kato, C. N.; Shinohara, A.; Hayashi, K.; Nomiya, K. *Inorg. Chem.* **2006**, *45*, 8108.
(44) Glasoe, P. K.; Long, F. A. *J. Phys. Chem.* **1960**, *64*, 188.

DOI: 10.1021/acs.inorgchem.6b00385
Inorg. Chem. XXXX, XXX, XXX−XXX